# FREE CONVECTIVE FLOW OF HEAT GENERATING/ABSORBING ON TRANSIENT NATURAL CONVECTION IN A VERTICAL CHANNEL: THE RIEMANN-SUM APPROACH

**BY**

**Abiodun O. Ajibade and Tafida M. Kabir**

*Department of Mathematics, Ahmadu Bello University, Zaria, Nigeria & Department of Mathematics, Federal College of Education, Zaria, Nigeria.*

*Corresponding author: mktafida.555@gmail.com*

## Abstract

*This article investigates the of heat generation/absorption on an unsteady free convective flow in channel formed by two vertical parallel plates. Equation of energy and momentum that describe the flow situations are solved using the Laplace transform method. Due to the difficulties that are associated with the analytical inversion of the obtained results from the Laplace to the time domain, the Riemann-Sum approach is employed to do the inversion, thus obtaining the temperature, velocity, skin-friction and rate of heat transfer. To validate the Riemann-sum approach used, the steady state solution for velocity and temperature are obtained analytically. An excellent agreement is found between the steady state solutions and the transient solutions at large values of time.*

**Keywords:** free convection; heat generation; suction/injection; Riemann-sum approximation.

## Nomenclature

| | | |
|---|---|---|
| $g$ | - | acceleration due to gravity [ms$^{-2}$] |
| $h$ | - | width of the channel [m] |
| $\Pr$ | - | Prandtl number |
| $H$ | - | dimensionless heat sink parameter |
| $t'$ | - | dimensional time |
| $t$ | - | dimensionless time |
| $T'$ | - | dimensional fluid temperature |
| $T_w'$ | - | channel wall temperature $(t' > 0)$ |
| $T_0'$ | - | initial temperature of fluid at $(t' \leq 0)$ |
| $T$ | - | dimensionless fluid temperature. |
| $u'$ | - | dimensional velocity [ms$^{-1}$] |
| $u$ | - | dimensionless velocity |
| $y'$ | - | co-ordinate perpendicular to the plate [m] |
| $y$ | - | dimensionless co-ordinate perpendicular to the plate |
| $\beta$ | - | coefficient of thermal expansion [K$^{-1}$] |
| $\mu$ | - | coefficient of viscosity [Kgm$^{-1}$s$^{-1}$] |
| $\upsilon$ | - | kinematic viscosity [m$^2$s$^{-1}$] |

## 1.0 Introduction

Investigations of convection heat and mass transfer, under the influence of heat generation/absorption and suction/injection have gained importance in many scientific and engineering applications. Such applications can be found in geothermal reservoir, nuclear reactor cooling, chemical catalytic, microelectronic devices, thermal insulation, geophysics, oceanography, environmental problems, energy conservation, underground disposal of nuclear waste material etc. Jha and Ajibade (2009) studied the influence of heat generation/absorption on free convective flow of viscous incompressible fluid between vertical porous plates due to periodic heating of the plates. They reported that heat absorption is to bring a decrease in the temperature and velocity of the fluid. Seth et al. (2010) investigated unsteady Hydromagnetic convective flow of a viscous incompressible electrically conducting heat generating/absorbing fluid within a parallel plate rotating channel in a uniform porous medium under slip boundary conditions. They observed that heat generation tends to accelerate fluid flow in both the primary and secondary flow directions whereas heat absorption has reverse effect on it. Siddiqa et al. (2010) studied natural convection flow of a viscous incompressible fluid over a semi infinite flat plate with the effects of exponentially varying temperature dependent viscosity and the internal heat generation. They concluded that an increasing values of heat generation parameter velocity increases and temperature decreases within the boundary layer. Magyari and Chamkha (2010) take into account the effect of heat generation to investigate the characteristics of heat and mass transfer in a micropolar fluid flow. Jha and Ajibade (2010a) analyzed time dependent natural convection Couette flow of heat generating/absorbing fluid which considered an accelerated motion of the channel plate. They showed that an increase in heat absorption parameter increases the rate of heat transfer on the accelerated plate and decreases the rate of heat transfer on the stationary plate. Ferdousi and Alim (2010) considered the effect of heat generation on natural convection flow from a porous vertical plate. Jha and Ajibade (2010b) analyzed unsteady free convective Couette flow of heat generating/absorbing fluid. Their conclusion shows that an increase in the heat absorption parameter decreases the skin friction on both the plates. Jha et al. (2011) investigated entropy generation under the effect of suction/injection. They findings reported that entropy generation number increases with suction on one porous plate and it decreases on the other porous plate with injection. Olanrewaju et al. (2012) studied internal heat generation effect on thermal boundary layer with convective surface boundary conditions. They showed that an increase in the internal heat generation prevent the rapid flow of heat from the lower surface to the upper surface of the plate. Kabir et al. (2013) examined effects of viscous dissipation on magnetohydrodynamics natural convection flow along a vertical wavy surface with heat generation. They discovered that velocity, temperature and skin friction coefficient enhance for higher values of internal heat generation parameter but the same reason the rate of heat transfer reduces. Daniel et al. (2013) investigated an unsteady forced and free convection flow past an infinite permeable vertical plate. They observed that thermal boundary layers increased towards the plate with injection and reduced towards the plate with suction and also seen that temperature is higher near the plate with injection while velocity is enhanced near the plate with suction and injection. Mostafa (2015) studied variable fluid properties effects on Hydromagnetic fluid flow over an exponentially stretching sheet. They observed that the local velocity Nusselt number increased with the increase of suction parameter, and heat generation parameter. Seth at al. (2015) analyzed unsteady Hydromagnetic natural convection flow of heat absorbing fluid within a rotating vertical channel in porous medium with Hall effects. They reported that heat absorption has tendency to reduce fluid temperature whereas fluid temperature is getting enhanced with the progress of time. Mohammed et al. (2015) examined effects of heat generation and thermal radiation on steady magnetohydrodynamics flow near stagnation point on a linear stretching sheet in porous medium and presence of variable thermal conductivity and mass transfer. They concluded temperature increases with an increase in the heat generation parameter. Jha et al. (2015) studied combined effects of suction/injection and wall surfaces curvature on natural convection flow in a vertical micro-porous annulus. They showed that suction/injection on the cylinder wall increases, the fluid velocity and temperature is enhanced. Halima et al. (2016) studied magnetohydrodynamics free convection flow with thermal radiation and chemical reaction effects in the presence of variable suction. Their outcomes showed that an increasing suction decrease the temperature profile of the fluid flow field at all points and also increase in suction decelerates the flow velocity.

The objective of the present article is to investigate the effect of free convective flow of heat generating/absorption in the channel using the Riemann-Sum approach.

## 2.0 Mathematical Analysis

Free convection flow of a viscous incompressible heat generating/absorbing fluid in a vertical channel of width $h$ is considered. The $X^{'}$-axis is taken along one of the porous channel walls while the $y^{'}$-axis is normal to it. The fluid was initially static and at the same temperature $T_0^{'}$ with the walls of the channel. At time $t^{'} > 0$, the temperature of the wall $y^{'} = 0$ becomes $T^{'} = T_w^{'}$ while the wall $y^{'} = h$ was kept at the temperature $T^{'} = T_0^{'}$. Natural convection sets in due to the temperature gradient. Because of the viscosity of the fluid consideration, the velocity of the fluid at both walls of the channel remains $u^{'} = 0$.

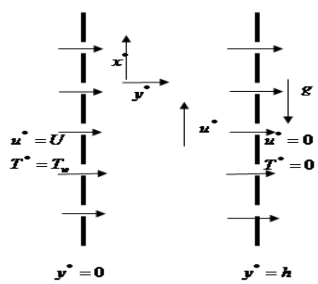


Fig. 1 Schematic diagram of the problem

By the use of Boussinesq's approximation, the governing equations for the flow problem in dimensionless form are:

$$\frac{\partial u}{\partial t} - q\frac{\partial u}{\partial y} = \frac{\partial^2 u}{\partial y^2} + T \quad (1)$$

$$\frac{\partial T}{\partial t} - q\frac{\partial T}{\partial y} = \frac{1}{\Pr}\frac{\partial^2 T}{\partial y^2} - \frac{H}{\Pr}T \quad (2)$$

The non-dimensional quantities introduced in the above equations are defined as:

$$t = \frac{t^{'}\upsilon}{h^2}, y = \frac{y^{'}}{h}, T = \frac{T^{'} - T_0^{'}}{T_w^{'} - T_0^{'}}, \Pr = \frac{\mu C_p}{k}, \; u = \frac{u^{'}\mu}{g\beta h^2 (T_w^{'} - T^{'})}, H = \frac{Q_0 h^2}{k} \quad (3)$$

The physical quantities used in the above equations are defined in the nomenclature. The initial conditions for velocity and temperature field in dimensionless form are:

$$u(0, y) = T(0, y) = 0, \;\; 0 \le y \le 1 \tag{4}$$

While the boundary conditions in dimensionless form is given as

$$t > 0 : \begin{cases} u = 0, T = 1, \, at \;\; y = 0 \\ u = 0, T = 0, \;\; at \;\; y = 1 \end{cases} \tag{5}$$

### 2.1 Solution by Laplace transform

Introducing the variables

$$\bar{u}(y,s) = \int_0^\infty u(y,t)\exp(-st)dt$$

$$\bar{T}(y,s) = \int_0^\infty T(y,t)\exp(-st)dt$$

Equations (1) and (2) are transformed using the initial condition (4) to

$$\frac{d^2\bar{u}}{dy^2} + q\frac{d\bar{u}}{dy} - s\bar{u} = -\bar{T} \tag{6}$$

$$\frac{d^2\bar{T}}{dy^2} + \delta\frac{d\bar{T}}{dy} - P\bar{T} = 0 \tag{7}$$

Where, $\delta = q\,\mathrm{Pr}$ and $P = (s\,\mathrm{Pr} + H)$

The boundary conditions (5) becomes

$$\bar{u} = 0, \bar{T} = \frac{1}{s} \;\text{ at }\; y = 0$$

$$\bar{u} = 0, \bar{T} = 0 \;\text{ at }\; y = 1$$

Using the method of undetermined coefficients, the solution of equations (6) and (7) under the boundary condition (8) can be written as

$$\bar{T} = c_1 \exp\left[y\left(\lambda - \frac{q\,\mathrm{Pr}}{2}\right)\right] + c_2 \exp\left[-y\left(\lambda + \frac{q\,\mathrm{Pr}}{2}\right)\right] \tag{9}$$

$$\bar{u} = d_1 \exp\left[y\left(\gamma - \frac{q}{2}\right)\right] + d_2 \exp\left[-y\left(\gamma + \frac{q}{2}\right)\right] + d_3 \exp\left[y\left(\lambda - \frac{q\,\mathrm{Pr}}{2}\right)\right] + d_4 \exp\left[-y\left(\lambda + \frac{q\,\mathrm{Pr}}{2}\right)\right] \tag{10}$$

Where

$$c_1 = \frac{\exp(-2\lambda)}{s[1-\exp(-2\lambda)]}, \;\; c_2 = \frac{1}{s[1-\exp(-2\lambda)]}, \;\; d_1 = -(d_2 + d_3 + d_4)$$

$$d_2 = \frac{(d_3 + d_4)\exp\left(\gamma - \frac{q}{2}\right) - d_3 \exp\left(\lambda - \frac{q\,\mathrm{Pr}}{2}\right) - d_4 \exp\left[-\left(\lambda + \frac{q\,\mathrm{Pr}}{2}\right)\right]}{\exp\left[-\left(\gamma + \frac{q}{2}\right)\right] - \exp\left(\gamma - \frac{q}{2}\right)}$$

$$d_3 = \frac{-c_1}{\left(\lambda - \frac{q\,\mathrm{Pr}}{2}\right)^2 + q\left(\lambda - \frac{q\,\mathrm{Pr}}{2}\right) - s}, \;\; d_4 = \frac{-c_2}{\left(\lambda + \frac{q\,\mathrm{Pr}}{2}\right)^2 - q\left(\lambda + \frac{q\,\mathrm{Pr}}{2}\right) - s}$$

$$\lambda = \sqrt{\frac{\delta^2}{4} + P}, \; \gamma = \sqrt{\frac{q^2}{4} + s}$$

By the use of equations (9) and (10), the skin-friction and the rate of heat transfer on the heated wall for $(y=0)$ are respectively

$$\tau_0 = \frac{d\bar{u}}{dy}|_{y=0} = d_1\left(\gamma - \frac{q}{2}\right) - d_2\left(\gamma + \frac{q}{2}\right) + d_3\left(\lambda - \frac{q\Pr}{2}\right) - d_4\left(\lambda + \frac{q\Pr}{2}\right) \tag{11}$$

$$Nu_0 = \frac{d\bar{T}}{dy}|_{y=0} = c_1\left(\lambda - \frac{q\Pr}{2}\right) - c_2\left(\lambda + \frac{q\Pr}{2}\right) \tag{12}$$

While at the isothermal wall $y=1$ the skin-friction and the rate of heat transfer are respectively

$$\tau_1 = \frac{d\bar{u}}{dy}|_{y=1} = d_1\left(\gamma - \frac{q}{2}\right)\exp\left(\gamma - \frac{q}{2}\right) - d_2\left(\gamma + \frac{q}{2}\right)\exp\left[-\left(\gamma + \frac{q}{2}\right)\right] + d_3\left(\lambda - \frac{q\Pr}{2}\right)\exp\left(\lambda - \frac{q\Pr}{2}\right)$$
$$- d_4\left(\lambda + \frac{q\Pr}{2}\right)\exp\left[-\left(\lambda + \frac{q\Pr}{2}\right)\right] \tag{13}$$

$$Nu_1 = \frac{d\bar{T}}{dy}|_{y=1} = c_1\left(\lambda - \frac{q\Pr}{2}\right)\exp\left(\lambda - \frac{q\Pr}{2}\right) - c_2\left(\lambda + \frac{q\Pr}{2}\right)\exp\left[-\left(\lambda + \frac{q\Pr}{2}\right)\right] \tag{14}$$

## 2.2 Riemann-Sum inversion of Laplace transform

This method inverts equations (9) to (13) in the $s$ domain to the time domain as follows:

$$U(y,t) = \frac{\exp(\varepsilon t)}{t}\left[\frac{1}{2}\bar{u}(y,\varepsilon) + \operatorname{Re}\sum_{n=1}^{N}(-1)^n \bar{u}\left(y, \varepsilon + \frac{in\pi}{t}\right)\right] \tag{15}$$

$$T(y,t) = \frac{\exp(\varepsilon t)}{t}\left[\frac{1}{2}\bar{T}(y,\varepsilon) + \operatorname{Re}\sum_{n=1}^{N}(-1)^n \bar{T}\left(y, \varepsilon + \frac{in\pi}{t}\right)\right] \tag{16}$$

$$\tau(y,t) = \frac{\exp(\varepsilon t)}{t}\left[\frac{1}{2}\bar{\tau}(y,\varepsilon) + \operatorname{Re}\sum_{n=1}^{N}(-1)^n \bar{\tau}\left(y, \varepsilon + \frac{in\pi}{t}\right)\right] \tag{17}$$

$$Nu(y,t) = \frac{\exp(\varepsilon t)}{t}\left[\frac{1}{2}\overline{Nu}(y,\varepsilon) + \operatorname{Re}\sum_{n=1}^{N}(-1)^n \overline{Nu}\left(y, \varepsilon + \frac{in\pi}{t}\right)\right] \tag{18}$$

Where

$\bar{U}(y,\varepsilon) = \bar{u}(y,s), \bar{T}(y,\varepsilon) = \bar{T}(y,s), \bar{\tau}(y,\varepsilon) = \bar{\tau}(y,s)$ and $\bar{Nu}(y,\varepsilon) = \bar{Nu}(y,s)$

$Re$ refers to the 'real part of', $i=\sqrt{-1}$ is the imaginary number, $N$ is the number of terms used in the Riemann-sum approximation and $\varepsilon$ is the real part of the Bromwich contour that is used in inverting Laplace transforms. The Riemann-sum approximation for the Laplace inversion involves a single summation for the numerical process. Its accuracy depends on the value of $\varepsilon$ and the truncation error dictated $N$ by (Tzou, 1997). According to Khadrawi and Al-Nimr (2007), for faster convergence, the quantity $\varepsilon t = 4.7$ gives the most satisfactory results since other tested values of $\varepsilon t$ selected need longer computational time.

## 2.3 Steady-state solution

To validate the Riemann-sum approximation used, the steady-state solutions for velocity and temperature fields are derived by taking $\frac{\partial(\ )}{\partial t} = 0$ in equations (1) and (2) which reduce to

$$\frac{d^2u}{dy^2}+q\frac{du}{dy}=-T \tag{19}$$

$$\frac{d^2T}{dy^2}+\delta\frac{dT}{dy}-HT=0 \tag{20}$$

These are solved analytically under the boundary conditions (5) to obtain the following steady-state solutions.

$$\bar{\bar{T}}=F_1\exp(my)+F_2\exp(ny) \tag{21}$$

$$\bar{\bar{u}}=\frac{-F_1\exp(my)}{m(m+q)}-\frac{F_2\exp(ny)}{n(n+q)}+\frac{F_3}{q}+F_4\exp(-qy) \tag{22}$$

$$\bar{\bar{\tau}}_0=\frac{d\bar{\bar{u}}}{dy}|_{y=0}=\frac{mF_1}{m(m+q)}-\frac{nF_2}{n(n+q)}-qF_4 \tag{23}$$

$$\bar{\bar{Nu}}_0=\frac{d\bar{\bar{T}}}{dy}|_{y=0}=mF_1+nF_2 \tag{24}$$

$$\bar{\bar{\tau}}_1=\frac{d\bar{\bar{u}}}{dy}|_{y=1}=\frac{mF_1\exp(m)}{m(m+q)}-\frac{nF_2\exp(n)}{n(n+q)}-qF_4\exp(-q) \tag{25}$$

$$\bar{\bar{N}}_1=\frac{d\bar{\bar{T}}}{dy}|_{y=1}=mF_1\exp(m)+nF_2\exp(n) \tag{26}$$

Where

$$F_1=\frac{-\exp(n)}{\exp(m)-\exp(n)},\quad F_2=\frac{\exp(m)}{\exp(m)-\exp(n)}$$

$$F_3=\frac{F_1q\exp(m)}{m(m+q)}+\frac{F_2q\exp(n)}{n(n+q)}-F_4q\exp(-q)$$

$$F_4=\frac{F_1(1-\exp(m))}{m(m+q)(1-\exp(-q))}+\frac{F_2(1=\exp(n))}{n(n+q)(1-\exp(-q))}$$

$$m=\frac{-\Pr q+\sqrt{(\Pr q)^2+4H}}{2},\quad n=\frac{-\Pr q-\sqrt{(\Pr q)^2+4H}}{2}$$

## 3.0 Results and discussions

The present work analyses the effect of heat generation on transient natural convection in a vertical channel using the Riemann-Sum approach. The velocity field, temperature field, Skin-friction and rate of heat transfer are presented graphically in figures 2-17 for various values of heat generation/absorption $(H)$, suction/injection $(q)$ and time $(t)$. For the purpose of this discussion, the parameters of interest are arbitrarily selected between $-2\le H\le 2$, $-2\le q\le 2$, $0.2\le t\le 1$ while the working fluid is considered to be air so that $\Pr=0.71$.

Figures 2 and 3 present the temperature and velocity profiles for different values of time respectively. It is clearly observed in figure 2 that fluid temperature increases with time and attains a steady-state for large values of time. This strengthens the convection current within the channel and it results to an increase in the fluid velocity shown in figure 3.

Figures 4 and 5 depict the effect of suction/injection on the fluid temperature and velocity. It should be noted that $q>0$ signifies suction on the heated plate with a corresponding injection on the cold plate. In this situation, it is observed that as suction increases on the heated plate, temperature within the channel responded with a decrease as shown in figure 3. This is physically expected since horizontal fluid motion is in the direction opposing the heat flux from the heated plate. The decrease in temperature weakens the convection current and as such, fluid velocity decreases as suction increases through the heated plate, when fluid is injected through the heated plate, horizontal fluid motion and heat flux to boost the fluid temperature in the channel. Hence the fluid temperature as well as velocity grow with increasing injection. This agrees well with the results of Jha and Ajibade (2009). In addition, it is observed that the effect of transpiration on fluid velocity is negligible at fluid sections close to the heated wall.

Figures 6 and 7 illustrate the effect of heat generation/absorption on the fluid temperature and velocity respectively. It is seen from the figures that as the heat generation $(H < 0)$ increases, fluid temperature and velocity increase while it decreases with increase in heat absorption $(H > 0)$. Increasing the heat generation parameter causes the fluid temperature to increase and it strengthens the convection current within the channel. In addition, increasing the heat absorption parameter causes a drop in fluid temperature and the thermal boundary layer becomes thinner thereby reduces the velocity distribution of the fluid as shown in figure 7.

Figures 8 and 9 show the temperature and velocity profiles for different value of Prandtl number $\Pr$. An obvious fact in figures 8 and 9 is that the fluid temperature and velocity decreases with the increase of Prandtl number $\Pr$. This is physically true because an increase in $\Pr$ decreases the thermal diffusivity of the working fluid. Consequently the temperature of the fluid decrease and as such, convection current is weakened leading to a decrease in velocity as shown in figure 9.

A clear view from figure 10 shows that as $\Pr$ increases, rate of heat transfer decreases on the cold plate. This is due to the fact that temperature decreases with increase in $\Pr$ (see figure 8), thus leading a decrease in the temperature gradient hence a decrease in the rate of heat transfer. In addition, as suction $(q)$ increases on the cold plate, rate of heat transfer is seen to linearly increase. It is further observed that heat transfer for fluids with higher $\Pr$ has a high rate of increase as suction grows on the cold plate. The reverse is observed in case of heated wall $(y = 1)$ as shown in figure 11. Comparisons between both plates show that heat transfer is higher on the cold plate in comparison to the heated plate.
Figures 12 and 13 depict the effect of heat source/sink on the rate of heat transfer at both walls $(y = 0, y = 1)$ in this situation, the heat source $(H < 0)$ decreases the rate of heat transfer on the heated wall, while it increases same on the cold wall $(y = 1)$. The reverse phenomenon is observed in case of heat sink $(H > 0)$. This is physically true since fluid temperature increases with heat source and this decreases the temperature gradient on the heated plate while heat transfer to the cold plate increases. The skin-friction on the heated plate is shown in figure 14 for different values of heat source/sink $(H)$. An observation from this figure indicates that the skin-friction increases with increase in heat source while it decreases with increase in heat sink.

Figure 15 shows that the skin-friction decreases as $\Pr$ increases. Physically, this is true because an increase in $\Pr$ decreases the velocity as shown in fig 9.

Figures 16 and 17 present the skin-friction at the both walls for different value of Prandtl number $\Pr$. A clear view from these figures is that on both walls as $\Pr$ increases skin-friction decreases. Physically, this is true because an increase in $\Pr$ decreases the velocity as shown in fig 9. However, skin-friction grows with increasing suction on the cold plate while it decreases on the hot plate as suction is increased on the cold plate $q > 0$.

Table 1 shows that transient temperature and velocity increase with increasing time and finally attains a steady state for large values of time which coincides with the steady state temperature and velocity.

Figures

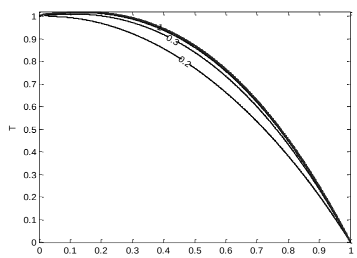

Fig. 2 Temperature profile for different value of time (Pr=0.71, H=-2.0, q=-2.0)

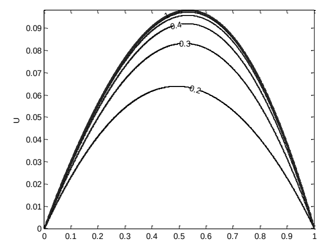

Fig. 3 Velocity profile for different value of time (Pr=0.71, H=-2.0,q=-2.0)

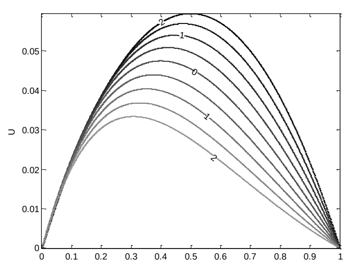

Fig. 5 Velocity profile for different value of q (Pr=0.71, t=0.3, H=2.0)

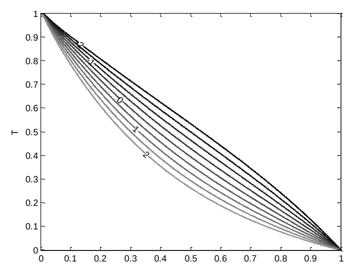

Fig. 4 Temperature profile for different value of q (Pr=0.71, t=0.3, H=2.0)

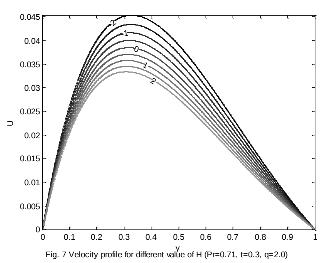


Fig. 7 Velocity profile for different value of H (Pr=0.71, t=0.3, q=2.0)

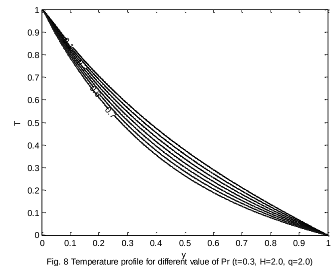


Fig. 8 Temperature profile for different value of Pr (t=0.3, H=2.0, q=2.0)

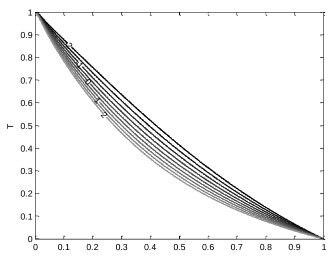


Fig. 6 Temperature profile for different value of H (Pr=0.71, t=0.3, q=2.0)

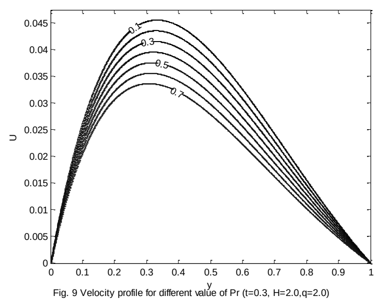


Fig. 9 Velocity profile for different value of Pr (t=0.3, H=2.0,q=2.0)

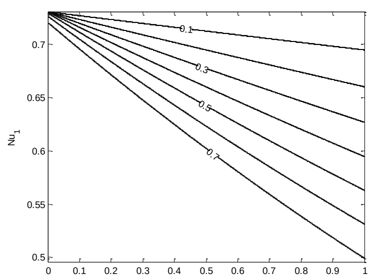


Fig. 11 Rate of heat transfer for Pr (t=0.3, H=2.0) at y=1

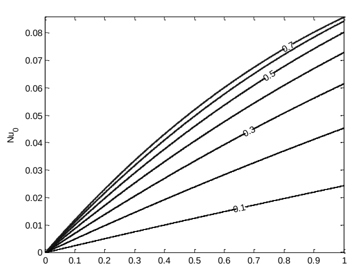


Fig. 10 Rate of heat transfer for Pr (t=0.3, H=2.0) at y=0

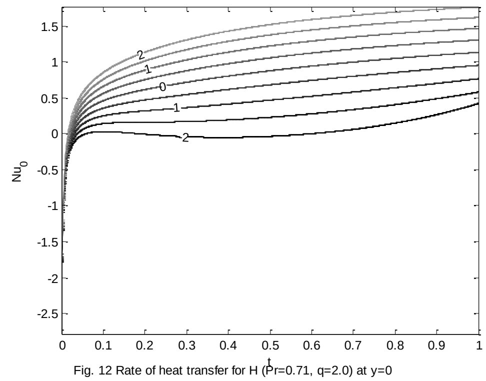

Fig. 12 Rate of heat transfer for H (Pr=0.71, q=2.0) at y=0

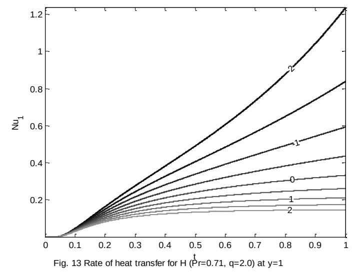

Fig. 13 Rate of heat transfer for H (Pr=0.71, q=2.0) at y=1

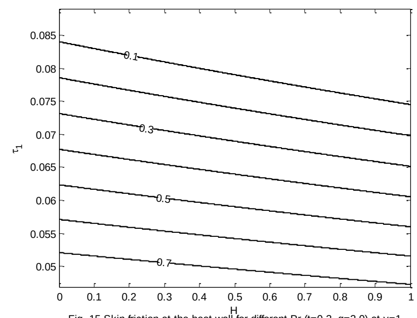

Fig. 15 Skin-friction at the heat wall for different Pr (t=0.3, q=2.0) at y=1

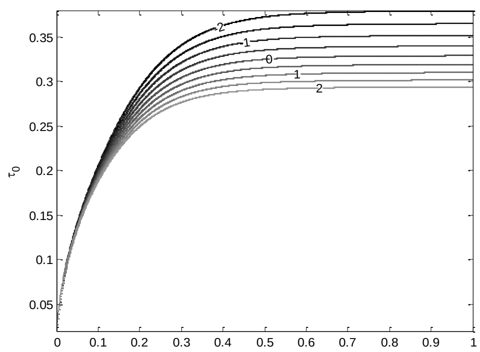

Fig. 14 Skin friction at the cold wall for different H (pr=0.71, q=2.0) at y=0

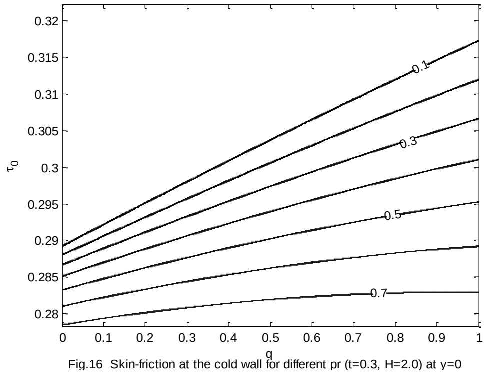

Fig.16 Skin-friction at the cold wall for different pr (t=0.3, H=2.0) at y=0

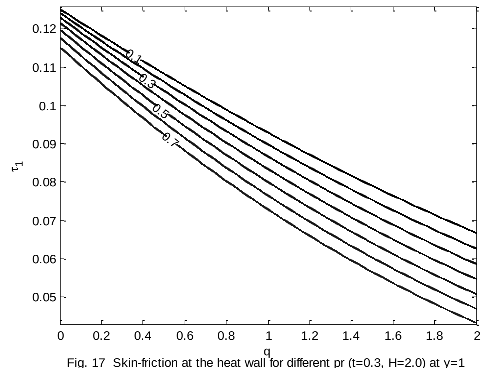

Fig. 17 Skin-friction at the heat wall for different pr (t=0.3, H=2.0) at y=1

Table1.

| Transient (using Riemann-Sum) | Temperature | Velocity |
|---|---|---|
| ***T*** | ***H = q = -2.0*** | |
| 0.1 | 0.5420 | 0.0293 |
| 0.3 | 0.8399 | 0.0829 |
| 0.5 | 0.8681 | 0.0951 |
| 0.7 | 0.8707 | 0.0971 |
| 0.8 | 0.8709 | 0.0973 |
| Steady state | 0.8709 | 0.0973 |

## 4. Conclusions

An analysis of the transient free convective flow of a viscous incompressible fluid in a vertical channel formed by two parallel porous plates in the presence of heat generation is considered. The Laplace transform method is used to solve the dimensionless governing linear partial differential equation. The conversion from the Laplace domain to the time domain is achieved by the Riemann-sum approximation method. The effects of governing parameters are studied. It has been found that fluid temperature and velocity increases with time and attains a steady-state for large values of time. In addition, fluid temperature and velocity increase on the heated plate, temperature within the channel responded with a decrease. Moreover, as the heat source increases, fluid temperature and velocity increase while it decreases with the increase in heat sink. The skin-friction increases with increase in heat source while it decreases with increase in heat sink. The rate of heat transfer decreases with increase in Prandtl number $(\text{Pr})$. Furthermore, heat source decreases the rate of heat transfer on the heated wall, while it increases same on the cold wall.

## REFERENCES


Daniel, S., Tella, Y., and Sani, U. (2013). An unsteady forced and free convection flow past an infinite permeable vertical plate. *International Journal of Science and Technology. 3(3).*

Ferdousi, A., and Alim, M. A. (2010). Natural convection flow from a porous vertical plate in the presence of heat generation. *D. Int. Uni. J. Sci. Tech.* ***5****(1): 73-80.*

Halima, U., Uwanta, I. J., and Samaila, K. A. (2010). Magnetohydrodynamics free convection fl-ow with thermal radiation and chemical reaction effects in the presence of variable suction. *MATEC Web of conferences. 64: 01002.*

Jha, B. K., and Ajibade, A. O. (2009). Considered the case of a free convective flow of heat generation/absorbing fluid between vertical parallel porous plates due to periodic heating on the porous plates. *International Communication Heat and Mass Transfer. 36, 624-631.*

Jha, B. K. and Ajibade., A. O. (2010a). Time dependent natural convection Couette flow of heat and generating/absorbing fluid. *International Journal of Applied Mechanics and Engineering. 15(4), (2010): 1083-1100.*

Jha, B. K. and Ajibade, A. O. (2010b). Unsteady free convective Couette flow of heat generating/ absorbing fluid. *International Journal of Energy and Technology. 2(12): 1-9.*

Jha, B. K., Ajibade., A. O., and Andrew, O. (2011). Entropy generation under the effect of suction /injection. *Applied Mathematical Modelling. 35(9): 4630 – 4646.*

Jha, B. K., Aina, B., and Muhammad, S. A. (2015). Combined effects of suction /injection and wa-ll surfaces curvature on natural convection flow in a vertical micro-porous annulus. *Therm-ophysics and Aeromechanics 22(2).*

Kabir, K. H., Alim.,M. A., and Andallah, L. S. (2013). Effects of viscous dissipation on magnetohy-drodynamics natural convection flow along a vertical wavy surface with heat generation. *American Journal of Computational methods 3: 91 – 98.*

Khadrawi, A. F., and Al-Nimr, M. A. (2007). Unsteady natural convection fluid flow in a vertical microchannel under the effect of the dual-phase-lag heat conduction model *Int. J. of Thermophysics, vol. 28, pp. 1387-1400.*

Magyari, E., and Chamkha, A. J. (2010). Combined effect of heat generation or absorption and first-order chemical reaction on micropolar fluid flows over a uniformly stretched permeable surface: The full analytical solution. *International Journal of thermal Science. 1 – 8.*

Mohammed, I. S., and Suneetha, K. (2015). Effects of heat generation and thermal radiation on steady magnetohydrodynamics flow near stagnation point on a linear stretching sheet in po-rous medium and presence of variable thermal conductivity and mass transfer. *Journal of C-omputational and Applied Research in Mechanical Engineering. 4(2): 133 – 144.*

Mostafa, A. A. M. (2015). Variable fluid properties effects on Hydromagnetic fluid flow over an exponentially stretching sheet. *Open Science Journal of Mathematics and application. 3(2): 26 – 33.*

Olarenwaju, P. O., Arulogun.,O. T., and Adebimpe, K. (2012). Internal heat generation effect on thermal boundary layer with convective surface boundary conditions. *American Journal of fluid Dynamics. 2(1): 1 – 4.*

Seth, G. S., Nandkeolyar, R., and Ansari, M. S. (2010). unsteady Hydromagnetic convective flow of a viscous incompressible electrically conducting heat generating/absorbing fluid within a parallel plate rotating channel in a uniform porous medium under slip boundary conditions. *International Journal Engineering Science and Technology. 2(11): 1-16.*

Seth, G. S., Kumbhhakar, B., and Sharmer, R. (2015). unsteady Hydromagnetic natural convect- on flow of heat absorbing fluid within a rotating vertical channel in porous medium with Hall effects. *International Journal of Heat and Technology 33(3): 139 – 144.*

Siddiqa, S., Asghar, S., and Hossain, M. A. (2010). Natural convection flow over an inclined Flat plate with internal heat generation and variable viscosity. *Math. Comp. Modelling 52: 1739-1751.*

Tzou D. Y. (1997). Macro to microscale heat transfer: The lagging behavior. Taylor and Francis